Journal of Environmental Chemical Engineering 3 (2015) 2597–2603

Contents lists available at ScienceDirect

Journal of Environmental Chemical Engineering

journal homepage: www.elsevier.com/locate/jece

Synthesis of novel Bi_2O_3–montmorillonite nanocomposite with enhanced photocatalytic performance in dye degradation

Sandip P. Patil[a], V.S. Shrivastava[a], G.H. Sonawane[b,*], S.H. Sonawane[c]

[a] Nano-Chemistry Research Laboratory, G.T. Patil College, Nandurbar 425 412, Maharashtra, India
[b] Deptartment of Chemistry, Kisan Arts, Commerce and Science College, Parola 425 111, Maharashtra, India
[c] Chemical Engineering Department, National Institute of Technology, Warangal 506004, TS, India

ARTICLE INFO

Article history:
Received 11 July 2015
Accepted 4 September 2015
Available online 9 September 2015

Keywords:
Bi_2O_3–montmorillonite
Congo red
Photocatalysis
Advanced oxidative process

ABSTRACT

Novel Bi_2O_3–montmorillonite nanocomposite photocatalyst was synthesized and characterized by scanning electron microscopy (SEM), energy dispersive X-ray spectroscopy (EDS) and X-ray diffraction (XRD). Effect of Bi_2O_3 intercalation with montmorillonite clay on photocatalytic performance of Bi_2O_3–montmorillonite under visible light irradiation was systematically investigated. The results indicate that Bi_2O_3–montmorillonite shows enhanced adsorption and photocatalytic performance for Congo red (CR) removal under visible light irradiation. Higher rate of light absorption and lower rate electron–hole pair recombination are responsible for the increase in photocatalytic efficiency. Adsorption of CR on Bi_2O_3–montmorillonite follows pseudo-second-order kinetics and the adsorption isotherm follows Freundlich isotherm. The monolayer capacity was observed to be 500 mg g^{-1}. The maximum percentage removal achieved upto 86.4% at pH 9 for 2 g L^{-1} photocatalyst dose. Photocatalytic degradation of CR by Bi_2O_3–montmorillonite proceeds via advanced oxidative process.

Introduction

Ever increasing development of dye industry causes dye pollution. It plays important role in increasing environmental pollution [1]. Their removal from wastewater is very difficult task [2]. Most of the conventional water treatment methods are ineffective for decolourization and degradation of the dyes from the wastewater [3–5]. These methods are also cost ineffective and sometimes partial oxidation of organic contaminants produces more toxic secondary pollutants than parent compounds [5,6]. Advanced oxidative processes (AOP) are the best alternative to the conventional methods for the complete and efficient degradation of the organic pollutants from the wastewater with considerable decrease in toxicity [6–8]. It includes set of various methods like Fenton and Fenton-like reactions, photo-Fenton and photo-Fenton-like reactions, ionizing radiations [9,10]. One of the AOPs is a photocatalysis process which involves generation of hydroxyl radicals that reacts with most of the organics and mineralizes them into CO_2, H_2O and inorganic ions [11].

Semiconductor based photocatalysts received much attention for the removal of dyes from wastewater. Out of these photocatalysts, TiO_2 based photocatalysts are most popular [12]. These are activated by UV light, which is only 2–3% of solar light. Therefore, researchers have been focusing their attention to develop visible light induced photocatalysts having a lower band gap.

Bi_2O_3 has a lower band gap 2.58–2.85 eV [13]. Thus, for the excitation of electron from valence band to conduction band requires visible light irradiations. Bi_2O_3 exhibits good photocatalytic efficiency for the removal of different dyes [14,15]. The natural clay like montmorillonite being inexpensive and easy availability, it is efficiently used for the removal of organic pollutants from wastewater by adsorption. Montmorillonite is consists of three-layered structural units, made up of two silica tetrahedral sheets and a central alumina octahedral sheet. The surface of montmorillonite can be used to prevent the guest particles from aggregation [16]. Efficiency of semiconductor based photocatalysts can be increased by incorporation into natural clays by forming nanocomposite materials [1,17]. These nanocomposites exhibits increasing photocatalytic efficiency due to their cation exchange capacity, basal space, larger surface area and adsorption–desorption property [18–20]. The intercalation of Bi_2O_3 with montmorillonite clay should be promising method to enhance photocatalytic performance of Bi_2O_3.

Present study involves incorporation of Bi_2O_3 semiconductor with montmorillonite clay to obtain Bi_2O_3–montmorillonite

* Corresponding author. Fax: +91 2597223688.
E-mail address: drgunvantsonawane@gmail.com (G.H. Sonawane).

http://dx.doi.org/10.1016/j.jece.2015.09.005
2213-3437/

nanocomposite. The resulting nanocomposites were characterized by SEM, EDS and XRD. The objective of this study is to investigate the photocatalytic degradation of CR in the presence of a visible light source and nano Bi_2O_3–montmorillonite as composite photocatalyst. The effect of the key operating parameters, viz. catalyst dosage, pH, initial dye concentration and contact time in the presence of visible light irradiation for the degradation of CR was studied. The removal of CR occurs by photocatalysis and adsorption.

Material and methods

All the chemicals used in the present study are of A.R. grade. Montmorillonite K 10 was procured from Sigma–Aldrich, India. Bismuth nitrate, cetyl trimethyl ammonium bromide (CTAB) and CR are procured from S.D. Fine Chemicals, India and are used as supplied without further purification.

Preparation of Congo red solution

CR is an anionic dye with molecular weight 696.68 g mol^{-1} (M.F. $C_{32}H_{22}N_6O_6S_2Na_2$). Stock solution (500 mg L^{-1}) of CR was prepared in distilled water. The experimental solutions of required concentrations are prepared by diluting stock solution with distilled water.

Synthesis of Bi_2O_3–montmorillonite nanocomposite

0.1 mmol $Bi(NO_3)_3{\cdot}5H_2O$ is dissolved in 20 mL nitric acid (1.5 M) to avoid hydrolyzation of Bi^{3+} ions by preventing precipitation of $BiONO_3$ [21–23], then 3 wt% of modified montmorillonite clay (montmorillonite clay can be modified by insertion of CTAB to increase the basal spacing) is added. The resulting mixture is sonicated for 30 min to obtain uniform suspension. Then dilute NaOH is added to this solution with continuous stirring for 30 min. Then Bi_2O_3–montmorillonite nanocomposites are obtained by successive centrifugation and dispersions in alcohol. Finally nanocomposites are dried under vacuum and calcinated at 400 °C for 3–4 h.

Characterization of nanocomposite

The SEM images were taken using the Hitachi S-4800 (Japan) FESEM. EDS analysis was performed by using Bruker X Flash 5030. The XRD pattern of the samples were measured on a Brucker D 8 Advance X-ray diffractometer (Germany) using monochromatized Cu Kα ($\lambda = 0.15418$ nm) radiation under 40 kV and 40 mA and scanning over the range of $10^\circ \leq 2\theta \leq 60^\circ$.

Adsorption experiment

To study the adsorption of CR on Bi_2O_3–montmorillonite, the CR dye solution is magnetically stirred with Bi_2O_3–montmorillonite in dark for 60 min to ensure adsorption–desorption equilibrium between the CR and Bi_2O_3–montmorillonite. Then changes in concentration of CR are determined by UV–vis double beam spectrophotometer (Systronics India model-2203) at $\lambda_{max} = 497$ nm. The amount of CR adsorbed on Bi_2O_3–montmorillonite is calculated by Eq. (1).

$$q_t = \frac{(C_o - C_t)V}{W} \quad (1)$$

where q_t (mg g^{-1}) is the adsorption capacity at time t; C_o (mg L^{-1}) and C_t (mg L^{-1}) are the initial CR concentration and the CR concentration at time t; V (L) is the initial volume of dye solution and W (g) is the amount of nanocomposite.

Photocatalytic experiment

Photocatalytic degradation of CR by Bi_2O_3–montmorillonite was carried out in a photocatalytic reactor having a 500 W halogen lamp. Cooling water jacket is used to maintain temperature inside the reactor. Different nanocomposite doses are added to the 50 mL dye solution (20–80 mg L^{-1}) and then placed in a photocatalytic reactor. At regular intervals, sufficient amount of sample was withdrawn and then after centrifugation changes in the dye concentration were determined by UV double beam spectrophotometer. The percentage removal of CR was calculated by Eq. (2).

$$\text{Percentage removal} = \left(\frac{C_o - C_t}{C_o}\right) \times 100 \quad (2)$$

Results and discussion

SEM and EDS analysis

Nano Bi_2O_3 has rod shape [24]. Fig. 1a shows the well dispersion of Bi_2O_3 nanorods over montmorillonite clay. This proves good combination between them and the existence of Bi_2O_3–montmorillonite nanocomposite. Such types of crystalline nanorods are absent in natural montmorillonite clay (Fig. 1b). Fig. 1c shows the elemental analysis of material surface obtained by electron dispersive X-ray spectroscopy (EDS). Fig. 1c shows that Bi_2O_3–montmorillonite contains O K (45.72%), Bi K (24.68%), Na K (4.79%), Si K (21.42%), Al K (2.78%), Mg K (0.45%) and Ca K (0.17%). Bi peaks are absent in EDS of montmorillonite while EDS of Bi_2O_3–montmorillonite micrograph shows the presence of peaks of Bi and O proves existence of Bi_2O_3 in the nanocomposite.

XRD analysis

The XRD patterns of Bi_2O_3, montmorillonite and Bi_2O_3–montmorillonite are shown in Fig. 2. The diffraction pattern of Bi_2O_3 shows major peaks at 2θ of 21.28°, 28.64°, 33.47° and 34.41°. The XRD peaks matches with the reported values [25]. XRD patterns of montmorillonite clay contain major peaks at 2θ of 18.94°, 23.28°, 25.77° and 34.06°. The XRD analysis indicates that all the diffraction peaks of Bi_2O_3 and` montmorillonite are present in XRD pattern of Bi_2O_3–montmorillonite nanocomposite.

Adsorption study

Effect of contact time and initial dye concentration

The effect of contact time on adsorption of CR by Bi_2O_3, montmorillonite and Bi_2O_3–montmorillonite is shown in Fig. 3. It indicates that adsorption of CR over Bi_2O_3–montmorillonite is faster than Bi_2O_3 and montmorillonite. The rate of adsorption is faster for first 30 min, then it attains equilibrium. The faster adsorption upto 30 min is due to availability of more number of sites for adsorption. Later on the repulsion between solute and bulk phase causes difficulties in occupying remaining sites. It results into lowering of adsorption rate.

Fig. 4 shows the effect of initial dye concentration on adsorption rate. It shows that as initial dye concentration increases then rate of adsorption also increases with contact time. The amount of dye adsorbed q_t increases from 14.54 to 66.36 mg g^{-1} as initial dye concentration increased from 20 mg L^{-1} to 80 mg L^{-1} with increase in the percentage removal from 72.7 to 82.9% for 1 g L^{-1} adsorbent dose.

Effect of pH

The pH of the dye solution plays significant role in photocatalytic degradation of the dye solution [26,27]. The effect of pH

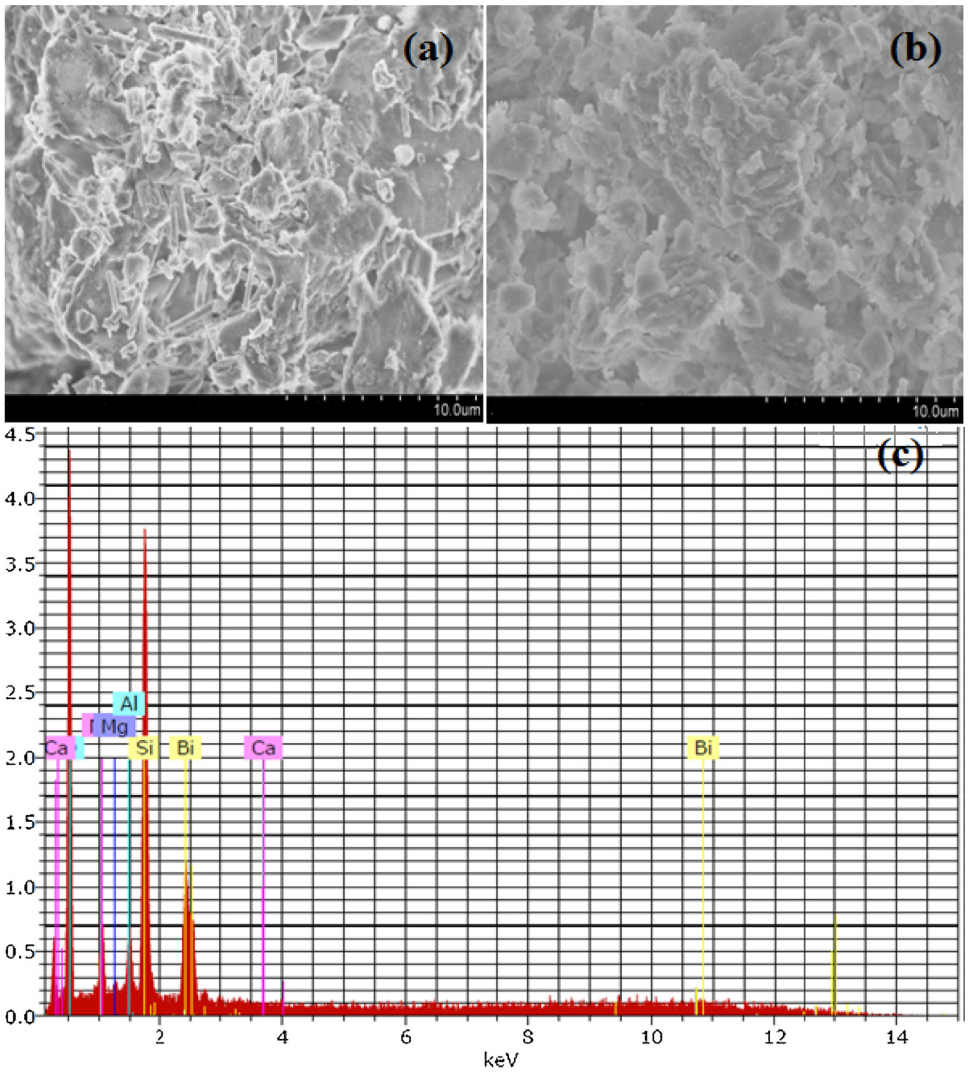

Fig. 1. The SEM images of (a) Bi_2O_3–montmorillonite and (b) montmorillonite. The EDS spectra of (c) Bi_2O_3–montmorillonite.

was investigated from pH 1 to 10 at 20 mg L^{-1} initial dye concentration for 1 g L^{-1} photocatalyst dose. It was observed that percent removal at pH 1 was 9.1%, then it increases upto 72.7% for pH 9 and again decreases on increase in pH. As pH increases from 1 to 9% removal also increases. To find out effect of pH on percentage removal of CR, zero point charge (ZPC) of the catalyst was determined. The ZPC of Bi_2O_3–montmorillonite was found to be 9.0. At the pH lower than ZPC, surface of Bi_2O_3–montmorillonite becomes positively charged. There is electrostatic attraction between positively charged Bi_2O_3–montmorillonite and anions of CR dye. Thus rate of adsorption of CR onto Bi_2O_3–montmorillonite surface is higher pH below ZPC.

Adsorption kinetics

Adsorption kinetics gives an idea about mechanism of adsorption. The adsorption kinetics of CR was studied with the help of pseudo-second-order model as given by Eq. (3) [28,29].

$$\frac{t}{q_t} = \frac{1}{K_2 q_e^2} + \frac{t}{q_e} \text{ and } h = K_2 q_e^2 \tag{3}$$

where K_2 is pseudo-second-order rate constant (g mg^{-1} min^{-1}), h is initial rate (mg g^{-1} min^{-1}). The linear plot of t/q_t vs t (Fig. 5) with regression coefficient $r^2 \geq 0.990$ shows good agreement with experimental q_e values (Table S1; Supplementary material). This indicates that adsorption of CR over Bi_2O_3–montmorillonite belongs to pseudo-second-order kinetics.

Adsorption isotherm

The linear form of Langmuir isotherm is represented as follows [1],

$$\frac{C_e}{q_e} = \frac{1}{ab} + \frac{C_e}{a} \tag{4}$$

where C_e is equilibrium concentration of dye, q_e is amount of dye adsorbed per unit mass of adsorbent (mg g^{-1}), a is monolayer coverage capacity (mg g^{-1}), b is Langmuir isotherm constant (L mg^{-1}). Langmuir isotherm describes homogeneous monolayer adsorption. Adsorption occurs at finite number of identical and equivalent sites without any interaction between the adsorbed molecules. Dimensionless factor or separation factor R_L values describes Langmuir adsorption isotherm whether adsorption is favourable, unfavourable, linear or irreversible. The present study reports value of R_L lies between 0 and 1 indicates favourable adsorption process (Table 1).

Linear form of Freundlich adsorption relationship is given as [30],

$$\log q_e = \log K_F + \frac{1}{n} \log C_e \tag{5}$$

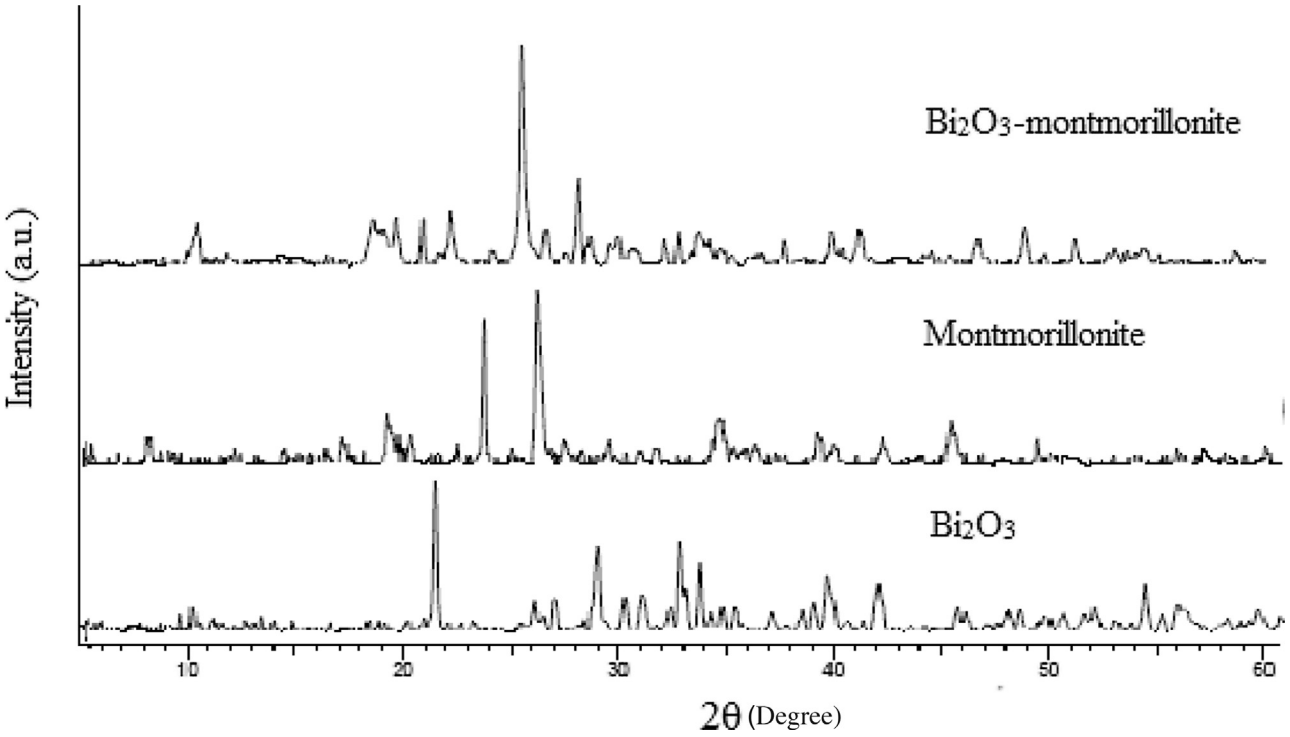

Fig. 2. XRD patterns of the montmorillonite, Bi_2O_3 and Bi_2O_3–montmorillonite.

where K_F is Freundlich isotherm constant $(mg\,g^{-1})\,(L\,g^{-1})^n$ related to adsorption capacity, C_e is equilibrium concentration of dye, $1/n$ is a measure of adsorption density or surface heterogeneity ranges between 0 and 1. Freundlich adsorption isotherm assumes heterogeneous, non-ideal, reversible and multilayer adsorption. Linear plot of log q_e vs log C_e (Fig. 6) shows applicability of Freundlich isotherm. Slope less than 1 indicates chemisorption; more than 1 indicates co-operative adsorption while closer to 0 indicates heterogeneity. The present study reports slope values more than 1 indicates adsorption of CR over Bi_2O_3–montmorillonite is co-operative adsorption (Table 1).

Freundlich isotherm has higher regression coefficient (r^2) and $1/n$ values while Langmuir isotherm has lower regression coefficient (r^2) values. Thus, Freundlich adsorption isotherm is the most appropriate isotherm for adsorption of CR on Bi_2O_3–montmorillonite.

Photocatalytic study

Photocatalytic performance of Bi_2O_3, montmorillonite and Bi_2O_3–montmorillonite was studied for the removal of CR (Fig. 7). The CR dye solutions along with catalyst are placed in a dark for 60 min to ensure adsorption–desorption equilibrium. It was then followed by photocatalytic degradation under visible light irradiation by considering time $t = 0$. The percent removal of CR by adsorption after 60 min using Bi_2O_3, montmorillonite and Bi_2O_3–montmorillonite are 10.2, 31.8 and 51.1%, respectively. This indicates that Bi_2O_3–montmorillonite has higher adsorption efficiency as compared to Bi_2O_3 and montmorillonite. It is reasonable to believe that when more organic molecules are adsorbed on the photocatalyst surface; the greater is the probability of the degradation.

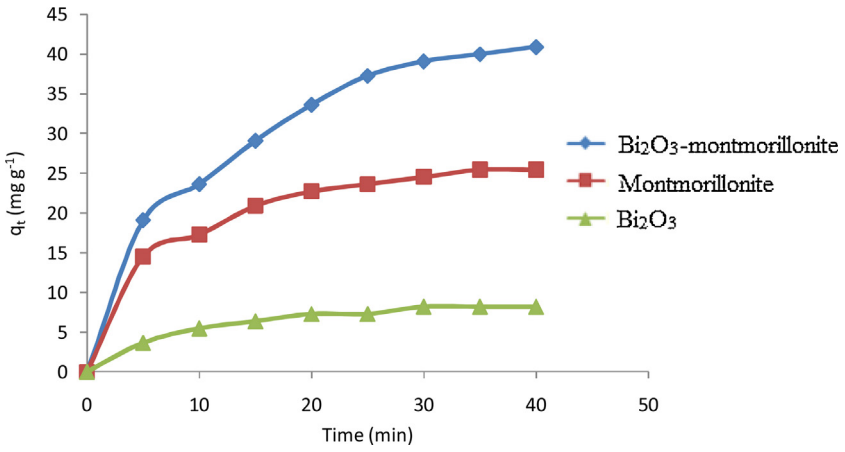

Fig. 3. Effect of contact time on adsorption of CR on montmorillonite, Bi_2O_3 and Bi_2O_3–montmorillonite.

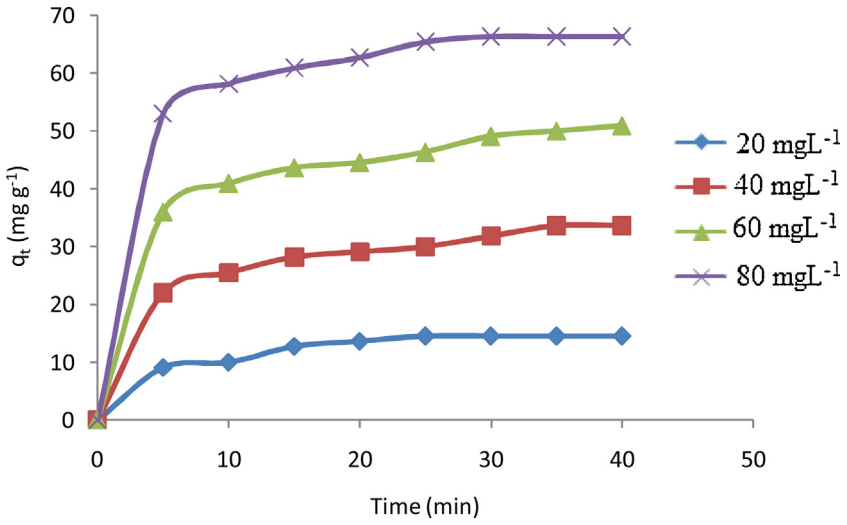

Fig. 4. Amount of dye adsorbed q_t (mg g^{-1}) with time for different initial CR dye concentration; pH 9, Bi_2O_3–montmorillonite dose 1 g L^{-1}.

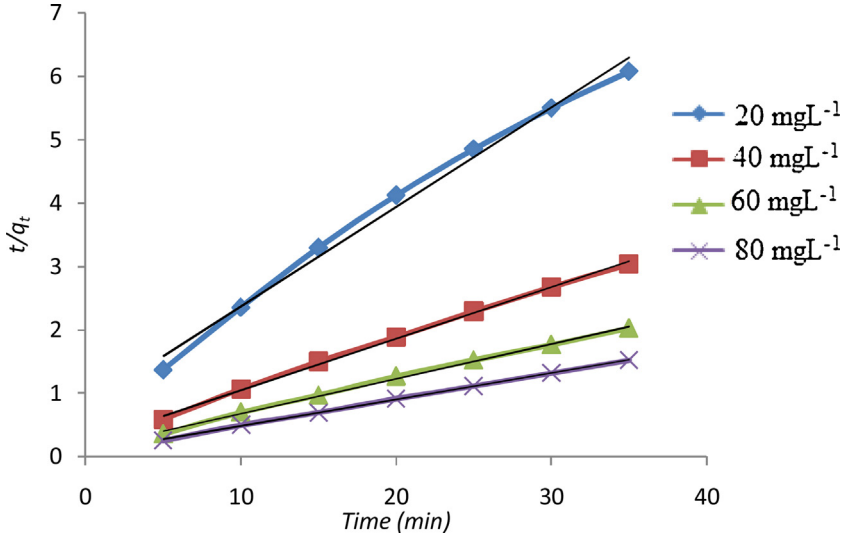

Fig. 5. Second-order kinetics plots for the removal of CR at different initial dye concentrations; Bi_2O_3–montmorillonite dose 3 g L^{-1}, pH 9.

After visible light irradiation for 35 min the removal of CR via photocatalytic degradation achieved by Bi_2O_3, montmorillonite and Bi_2O_3–montmorillonite 55.7, 34.1 and 82.9%, respectively. This exhibit that in the removal of CR, photocatalytic degradation was the dominant process than adsorption.

Degradation of CR can be explained on the basis of AOP by heterogeneous photocatalysis. AOP involves generation of electron–hole pair. They are again generates $O_2^{-\bullet}$ and $^{\bullet}OH$ radicals, respectively. These radicals are highly reactive and responsible for oxidative degradation of CR. While photogenerated hydrogen atom from water is responsible for reductive degradation [17]. Alcohols, like methanol and isopropanol are commonly used as scavengers for $^{\bullet}OH$ mediated degradation mechanisms [31,32]. Though direct oxidation of small aliphatic alcohols by photogenerated holes probably happens, it is negligible thus it is omitted. Present study involves use of isopropanol as scavenger. Fig. 8 shows that photodegradation of CR decreases to 59.1% in presence of i-PrOH as compare to photodegradation carried out in aqueous medium (86.4%). Decrease in percent removal indicates that $^{\bullet}OH$ radicals acts as predominant species in photocatalytic degradation of CR than $O_2^{-\bullet}$.

Table 1
Freundlich and Langmuir isotherm constants for adsorption of CR on Bi_2O_3–montmorillonite for different dye concentration and photocatalyst dose of 0.2–2 g L^{-1} at pH 9; contact time 30 min.

Dye concentration (mg L^{-1})	Freundlich coefficient				Langmuir coefficient			
	K_F (L g^{-1})	n	$1/n$	r^2	a (mg g^{-1})	b (g L^{-1})	R_L	r^2
20	4.3351	0.999	1.002	0.970	23.26	0.0804	0.3834	0.983
40	3.6813	0.998	1.001	0.923	200.00	0.0235	0.5155	0.832
60	1.4355	0.719	1.390	0.978	500.00	0.0097	0.6321	0.929
80	0.6950	0.605	1.652	0.980	166.67	0.0526	0.1920	0.941

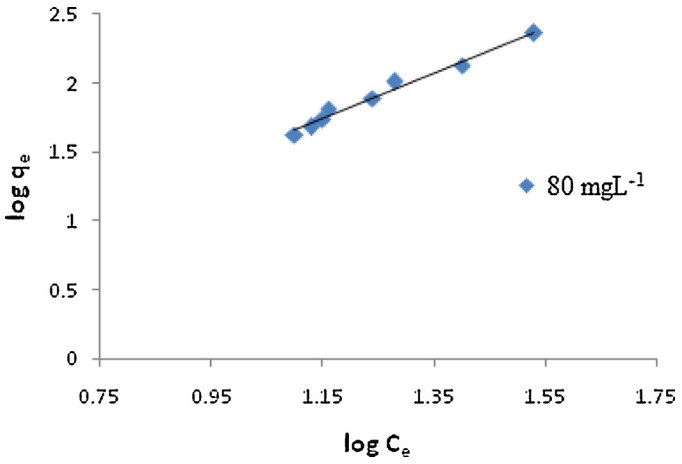

Fig. 6. Freundlich plot for adsorption of CR by Bi_2O_3–montmorillonite.

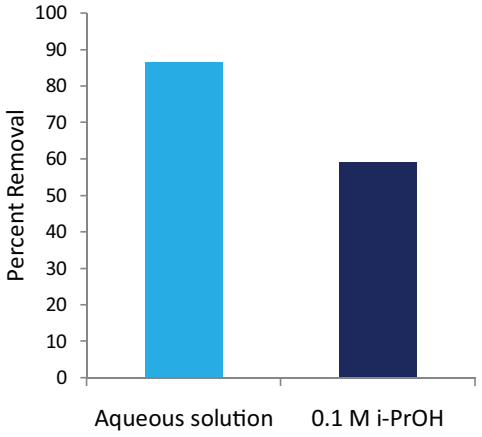

Fig. 8. Photocatalytic degradation of CR with addition of 0.1 M i-PrOH.

To confirm the stability of the high photocatalytic performance of the Bi_2O_3–montmorillonite nanocomposite, the recyclability of the Bi_2O_3–montmorillonite in the photocatalytic degradation of CR under visible light irradiation were investigated. To study its recyclability, the powdered nanocomposite was allowed to settle by gravity after the photocatalytic degradation. The recovered nanocomposite was then collected and reused for 2 times under same photodegradation conditions. Fig. 9 shows removal of CR by Bi_2O_3–montmorillonite after the 1st run achieved upto 86.4% after 30 min. After the 3rd run, removal of CR decreases down to 74.9%. Loss of the recycled catalyst during sampling is responsible for the decrease in the removal of CR. Fig. 9 shows that Bi_2O_3–montmorillonite has excellent stability and does not show significant loss in its activity after 3 cycling runs. This reflects that Bi_2O_3–montmorillonite does not suffer from photo-corrosion during degradation. This indicates the practical applicability of the Bi_2O_3–montmorillonite nanocomposite for the photocatalytic degradation of the CR dye.

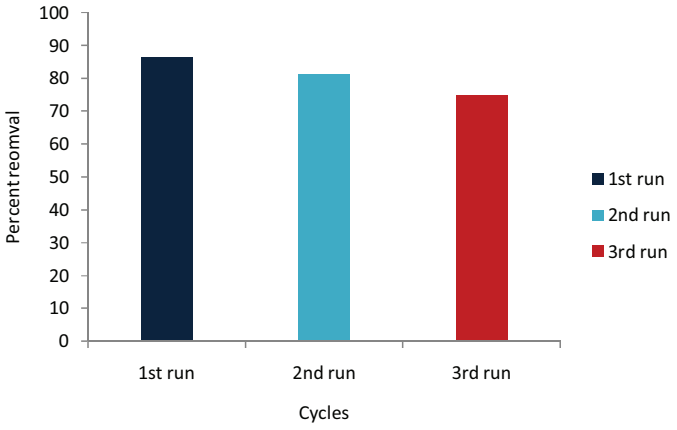

Fig. 9. Recycling performance of the Bi_2O_3–montmorillonite.

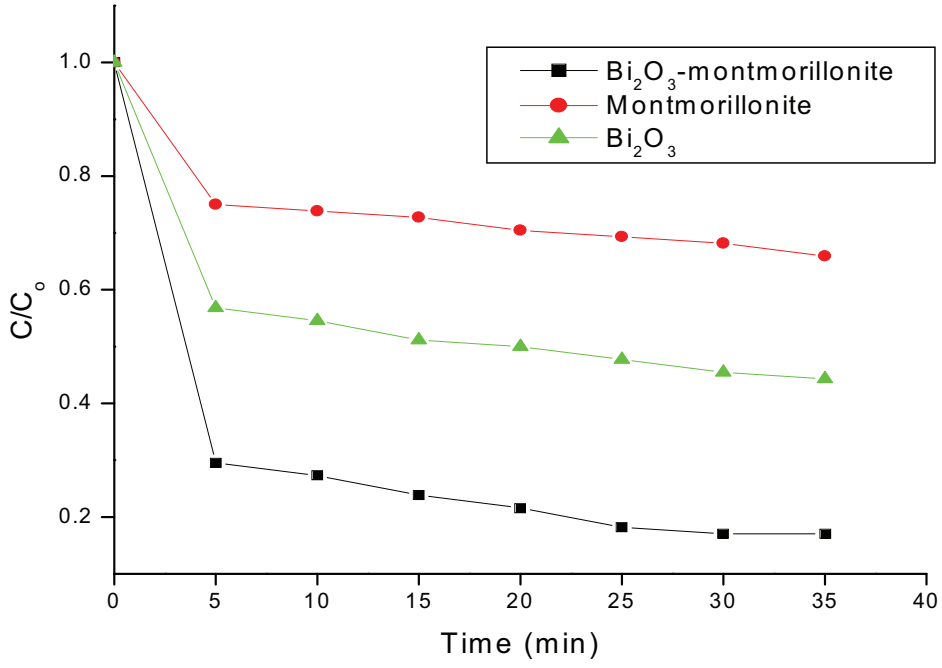

Fig. 7. Photocatalytic degradation of CR (80 mg L^{-1}) with Bi_2O_3, montmorillonite and Bi_2O_3–montmorillonite.

Conclusion

Bi_2O_3–montmorillonite nanocomposites have been successfully synthesized by sonochemical method. The Bi_2O_3–montmorillonite exhibits good photocatalytic efficiency for the photocatalytic degradation of CR in presence of visible light irradiation. Improvement in photocatalytic activity was observed when Bi_2O_3 was incorporated with montmorillonite clay by intercalation method. Improvement in photocatalytic activity was due to decrease in recombination of photo electron–hole pair and combined effect of adsorption and photocatalytic degradation. The adsorption kinetics follows pseudo-second-order kinetics, while adsorption isotherm follows Freundlich isotherm. The separation factor R_L in the present study reveals favourable adsorption process. The study of photocatalytic mechanism shows OH radicals, acts as the predominant species in photocatalytic degradation of CR than $O_2^{-\bullet}$ suggesting oxidative mineralization. Furthermore, the novel Bi_2O_3–montmorillonite nanocomposites with high mineralization efficiency, high stability and recyclability could be the potential material for the wastewater treatment on an industrial scale.

Acknowledgements

The authors gratefully acknowledges to Central Instrumentation Centre, University Institute of Chemical Technology, NMU, Jalgaon for providing SEM, EDX and XRD analysis. Authors are also thankful to Principal, Kisan College, Parola and Principal, G.T.P. College, Nandurbar for providing necessary laboratory facilities.

Appendix A. Supplementary data

Supplementary data associated with this article can be found, in the online version, at http://dx.doi.org/10.1016/j.jece.2015.09.005.

References

[1] S.P. Patil, V.S. Shrivastava, G.H. Sonawane, Photocatalytic degradation of Rhodamine 6G using ZnO–montmorillonite nanocomposite: a kinetic approach, Desalin. Water Treat. 54 (2015) 374–381.
[2] S. Vadivel, M. Vanitha, A. Muthukrishnaraj, N. Balasubramanian, Graphene oxide–BiOBr composite material as highly efficient photocatalyst for degradation of methylene blue and rhodamine-B dyes, J. Water Process Eng. 1 (2014) 17–26.
[3] X. Li, Q. Wang, Y. Zhao, W. Wu, J. Chen, H. Meng, Green synthesis and photocatalytic performances for ZnO-reduced graphene oxide nanocomposites, J. Colloid Interface Sci. 411 (2013) 69–75.
[4] C. Yu, F. Cao, G. Li, R. Wei, J.C. Yu, R. Jin, Q. Fan, C. Wang, Novel noble metal (Rh, Pd, Pt)/BiOX (Cl, Br, I) composite photocatalysts with enhanced photocatalytic performance in dye degradation, Sep. Purif. Technol. 120 (2013) 110–122.
[5] S. Dong, Y. Cui, Y. Wang, Y. Li, L. Hu, J. Sun, J. Sun, Designing three-dimensional acicular sheaf shaped $BiVO_4$/reduced graphene oxide composites for efficient sunlight-driven photocatalytic degradation of dye wastewater, Chem. Eng. J. 249 (2014) 102–110.
[6] M. Iqbal, Cytotoxicity and mutagenicity evaluation of gamma radiation and hydrogen peroxide treated textile effluents using bioassays, J. Environ. Chem. Eng. 3 (2015) 1912–1917.
[7] B. Neppolian, A. Bruno, C.L. Bianchi, M. Ashokkumar, Graphene oxide based Pt–TiO_2 photocatalyst: ultrasound assisted synthesis, characterization and catalytic efficiency, Ultrason. Sonochem. 19 (2012) 9–15.
[8] A. Aleboyeh, Y. Moussa, H. Aleboyeh, The effect of operational parameters on UV/H_2O_2 decolourization of Acid Blue 74, Dyes Pigm. 66 (2005) 129–131.
[9] M. Iqbal, I.A. Bhatti, Gamma radiation/H_2O_2 treatment of a nonylphenol ethoxylates: degradation, cytotoxicity, and mutagenicity evaluation, J. Hazard. Mater. 299 (2015) 351–360.
[10] K. Qureshi, M.Z. Ahmad, I.A. Bhatti, M. Iqbal, A. Khan, Cytotoxicity reduction of wastewater treated by advanced oxidation process, Chem. Int. 1 (2015) 53–59.
[11] E. Basturk, M. Karatas, Decolorization of anthraquinone dye Reactive Blue 181 solution by UV/H_2O_2 process, J. Photochem. Photobiol. A 299 (2015) 67–72.
[12] S.U.M. Khan, M. Al-Shahry, W.B. Ingler, Efficient photochemical water splitting by a chemically modified n-TiO_2, Science 297 (2002) 2243–2245.
[13] X. Liu, L. Pan, T. Lv, Z. Sun, C.Q. Sun, Visible light photocatalytic degradation of dyes by bismuth oxide-reduced graphene oxide composites prepared via microwave-assisted method, J. Colloid Interface Sci. 408 (2013) 145–150.
[14] S. Anandan, G.-J. Lee, P.-K. Chen, C. Fan, J.J. Wu, Removal of Orange II dye in water by visible light assisted photocatalytic ozonation using Bi_2O_3 and Au/Bi_2O_3 nanorods, Ind. Eng. Chem. Res. 49 (2010) 9729–9737.
[15] C. Pan, Y. Yan, H. Li, S. Hu, Synthesis of bismuth oxide nanoparticles by a templating method and its photocatalytic performance, Adv. Mater. Res. 557–559 (2012) 615–618.
[16] N. Khaorapapong, N. Khumchoo, M. Ogawa, Preparation of zinc oxide–montmorillonite hybrids, Mater. Lett. 65 (2011) 657–660.
[17] S. Meshram, R. Limaye, S. Ghodke, S. Nigam, S. Sonawane, R. Chikate, Continuous flow photocatalytic reactor using ZnO–bentonite nanocomposite for degradation of phenol, Chem. Eng. J. 172 (2011) 1008–1015.
[18] S. Sonawane, P. Chaudhari, S. Ghodke, S. Ambade, S. Gulig, A. Mirikar, A. Bane, Combined effect of ultrasound and nanoclay on adsorption of phenol, Ultrason. Sonochem. 15 (2008) 1033–1037.
[19] S.R. Shirsath, A.P. Hage, M. Zhou, S.H. Sonawane, M. Ashokkumar, Ultrasound assisted preparation of nanoclay bentonite–FeCo nanocomposite hybrid hydrogel: a potential responsive sorbent for removal of organic pollutant from water, Desalination 281 (2011) 429–437.
[20] U. Riaz, S.M. Ashraf, A. Ruhela, Catalytic degradation of orange G under microwave irradiation with a novel nanohybrid catalyst, J. Environ. Chem. Eng. 3 (2015) 20–29.
[21] H. Zhang, Y.J. Ji, X.Y. Ma, J. Xu, D.R. Yang, Long Bi_2S_3 nanowires prepared by a simple hydrothermal method, Nanotechnology 14 (2003) 974–977.
[22] A.P. Zhang, J.Z. Zhang, N.Y. Cui, X.Y. Tie, Y.W. An, L.J. Li, Effects of pH on hydrothermal synthesis and characterization of visible-light-driven $BiVO_4$ photocatalyst, J. Mol. Catal. A: Chem. 304 (2009) 28–32.
[23] X. Liu, L. Pan, T. Lv, Z. Sun, C.Q. Sun, Visible light photocatalytic degradation of dyes by bismuth oxide-reduced graphene oxide composites prepared via microwave-assisted method, J. Colloid Interface Sci. 408 (2013) 145–150.
[24] H.-Y. Jiang, K. Cheng, J. Lin, Crystalline metallic Au nanoparticle-loaded α-Bi_2O_3 microrods for improved photocatalysis, Phys. Chem. Chem. Phys. 14 (2012) 12114–12121.
[25] M. Anilkumar, Renu Pasricha, V. Ravi, Synthesis of bismuth oxide nanoparticles by citrate gel method, Ceram. Int. 31 (2005) 889–891.
[26] M. Shang, W. Wang, L. Zhang, Preparation of BiOBr lamellar structure with high photocatalytic activity by CTAB as Br source and template, J. Hazard. Mater. 167 (2009) 803–809.
[27] U.G. Akpan, B.H. Hameed, Parameters affecting the photocatalytic degradation of dyes using TiO_2-based photocatalysts: a review, J. Hazard. Mater. 170 (2009) 520–529.
[28] N.K. Amin, Removal of direct blue-106 dye from aqueous solution using new activated carbons developed from pomegranate peel: adsorption equilibrium and kinetics, J. Hazard. Mater. 165 (2009) 52–62.
[29] C. Kannan, K. Muthuraja, M.R. Devi, Hazardous dyes removal from aqueous solution over mesoporous aluminophosphate with textural porosity by adsorption, J. Hazard. Mater. 244–245 (2013) 10–20.
[30] Q. Manzoor, R. Nadeem, M. Iqbal, R. Saeed, T.M. Ansari, Organic acids pretreatment effect on Rosa bourbonia phyto-biomass for removal of Pb(II) and Cu (II) from aqueous media, Bioresour. Technol. 132 (2013) 446–452.
[31] X. Xiao, R. Hao, M. Liang, X. Zuo, J. Nan, L. Li, W. Zhang, One-pot solvothermal synthesis of three-dimensional (3D) BiOI/BiOCl composites with enhanced visible-light photocatalytic activities for the degradation of bisphenol-A, J. Hazard. Mater. 233–234 (2012) 122–130.
[32] C. Xu, H. Wu, F.L. Gu, Efficient adsorption and photocatalytic degradation of Rhodamine B under visible light irradiation over BiOBr/montmorillonite composites, J. Hazard. Mater. 275 (2014) 185–192.